

ANISOTROPY OF SURFACE TENSION AT THE BOUNDARY BETWEEN THE SUPERCONDUCTING AND NORMAL PHASES OF TIN

Yu. V. SHARVIN and V. F. GANTMAKHER

Institute for Physical Problems of the Academy of Sciences, U.S.S.R.

Submitted to JETP editor December 31, 1959

J. Exptl. Theoret. Phys. (U.S.S.R.) **38**, 1456-1470 (May, 1960)

The anisotropy of surface tension at the boundary between the *s* and *n* phases of tin was investigated by two methods. In the first, the structures of the intermediate state, revealed by using a ferromagnetic powder, were observed in specimens with different crystal orientations. In the second method, the moment of the forces acting on a spherical specimen in a magnetic field was measured. There was agreement between the results obtained by both methods. The form of the dependence of surface tension on the direction of the normal to the phase interface, the absolute order of magnitude of the effect and its temperature dependence were determined.

THERE is little known at present about the anisotropy of the properties of superconductors. In particular, the anisotropy of surface tension Δ^* at the boundary between the superconducting (*s*) and normal (*n*) phases has not been studied. A comparison between the anisotropy of Δ and the anisotropy of other quantities characterizing the electronic state of a metal is interesting, in that the method of studying the anisotropy of Δ has some advantages over the study of the anisotropy of other parameters of superconductors.

The boundary separating the *s* and *n* phases extends into the body of the metal. In studying Δ , therefore, we do not encounter the difficulties met in measuring the penetration depth of a magnetic field into a superconductor and the high-frequency impedance, where the results depend appreciably on the state of the surface of the metal.

On the other hand, we should point out that in measuring Δ the specimens must satisfy stringent requirements as to the perfection of the crystal lattice. It is essential that the phase boundary be able to move freely and take up the position corresponding to thermodynamic equilibrium. This condition gives rise to serious difficulties in the case of boundary movement in a solid. Any irregularities in the metal lattice give rise to "dry friction" in the movement of an *ns* boundary, i.e. to forces preventing the

motion of the boundary, which do not tend to zero as the movement slows down.

In our work we were up against the fact that in single-crystal tin with less than $6 \times 10^{-5}\%$ impurity, treated with the greatest care to avoid mechanical deformation, these forces nevertheless do not disappear and noticeably affect the regularity and reproducibility of the structures of the intermediate state. The form of the structures always depends, to a known extent, on the previous history of the specimen, i.e., on how the magnetic field and temperature were changed in the preceding moments.

This made investigation of the anisotropy of Δ considerably more difficult, especially as it turned out to be relatively small.

In order to obtain a qualitative picture of the phenomenon, we used two independent differential methods, which allowed direct comparison to be made between the values of Δ for different orientations of the *ns* boundary, under conditions which excluded, as far as possible, the influence of "dry friction" on the results.

1. THE "FROZEN-IN FLUX" METHOD

The object of this part of the work was to obtain information on the anisotropy of Δ from an analysis of the structures of the intermediate state, which can easily be observed by sprinkling a fine ferromagnetic powder on the surface of the specimen.^{1,2} The existence of an anisotropy in Δ should lead to a preferential orientation of the phase boundaries along directions for which Δ is

*We denote by Δ , as usual, a quantity with the dimensions of length, which is related to the magnitude of the surface free energy σ_{ns} by the relation $\sigma_{ns} = \Delta H_C^2 / 8\pi$.

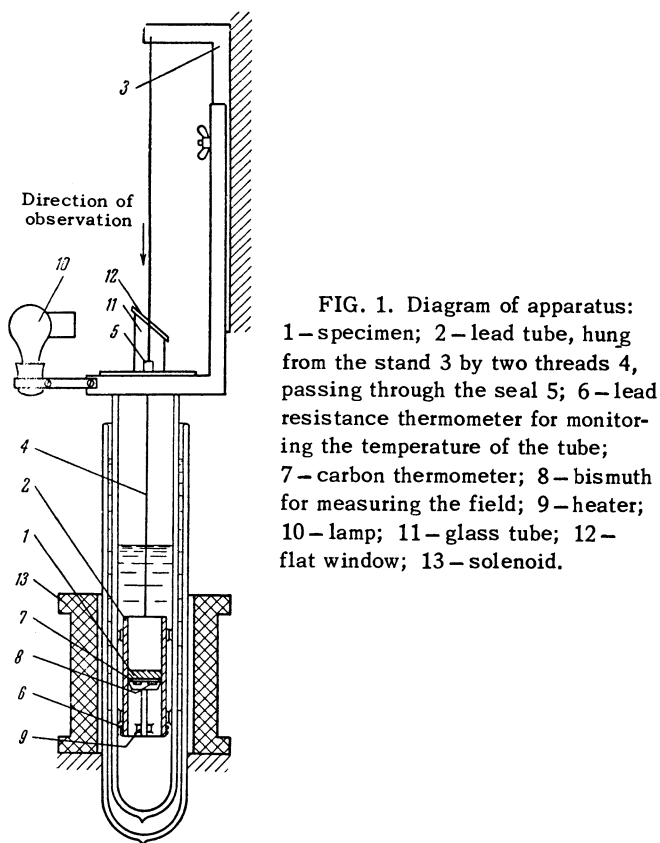


FIG. 1. Diagram of apparatus: 1—specimen; 2—lead tube, hung from the stand 3 by two threads 4, passing through the seal 5; 6—lead resistance thermometer for monitoring the temperature of the tube; 7—carbon thermometer; 8—bismuth for measuring the field; 9—heater; 10—lamp; 11—glass tube; 12—flat window; 13—solenoid.

a minimum, assuming of course that other factors that determine the arrangement of *s* and *n* domains are sufficiently unimportant.

First of all it is essential to remove all factors, related to the geometry of the field or of the specimen, which could affect the arrangement of the regions. Ideally the experiment would be carried out on an infinite plane-parallel plate of superconductor, in a uniform magnetic field perpendicular to its surface. We realized this case in practice by containing the specimen (a flat round single crystal of tin, 37 mm in diameter and 10 mm thick) — in a long lead tube (16 cm long) fitting the specimen closely (see Fig. 1). Since the critical field is considerably higher for lead than for tin at all temperatures, the lead tube acted as an ideal "magnetic mirror", thanks to which the specimen was equivalent to an infinite disc in an electrodynamic sense.

The uniform magnetic field, produced by a solenoid, penetrated the lead tube when its temperature was above the critical temperature for lead. A Dewar with liquid helium, which could be moved vertically, was first placed in its lower position. The Dewar was then raised, the lead tube immersed in the helium and cooled, and the magnetic flux became "frozen" in the tube. On lowering the temperature further (by pumping

the helium) the tin specimen went over into the intermediate state. As the magnetic flux in the specimen stayed constant, the transition occurred under the condition $B = \text{const}$ (B is the magnetic induction in the specimen, averaged over the volume, which contained a considerable number of *s* and *n* domains). It was essential for our purpose that this condition be fulfilled, since eddy currents would otherwise be induced on the surface of the specimen at the moment of transition, flowing round the whole specimen and exerting an orienting action on the position of the boundaries. It is known that this effect causes a marked 'radial' structure to appear in a spherical or plane cylindrical specimen when a field is suddenly trapped.^{3,1} In our case the edge and center of the specimen were in practically the same states, and no radial structures were observed.

The technique for introducing the ferromagnetic powder was the same as in the previous work² (the apparatus for sprinkling is not shown in Fig. 1). The illumination of the surface of the specimen was produced by an opal bulb, the light from which was reflected from the mirror surface of the specimen.

We obtained photographs of the structures of the intermediate state for nine tin single-crystal specimens, containing not more than $10^{-4}\%$ impurity. The crystallographic orientations of the specimens are shown in Fig. 2. Most of the pictures were taken at 3°K, and for some specimens the temperature dependence of the structures was followed up to 3.6°. The concentration C_S of the superconducting phase in the specimen was determined from the value of the frozen-in field B by the relation $C_S = 1 - B/H_C$.

The most convenient structures for interpretation were obtained with concentrations C_S in the range 0.05 – 0.2. The *s* domains then appeared

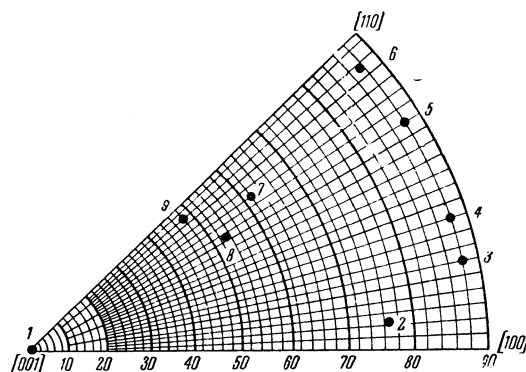


FIG. 2. Stereographic projection of the directions of the normals to the plane surfaces of the specimens.

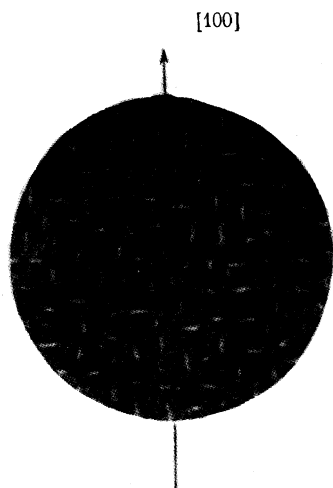


FIG. 3

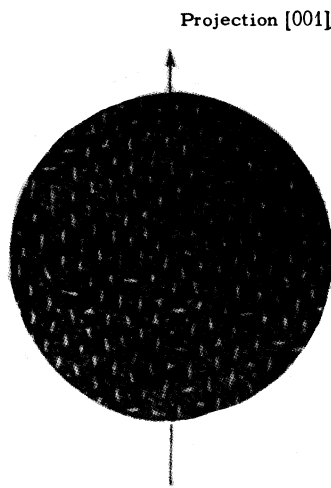


FIG. 4

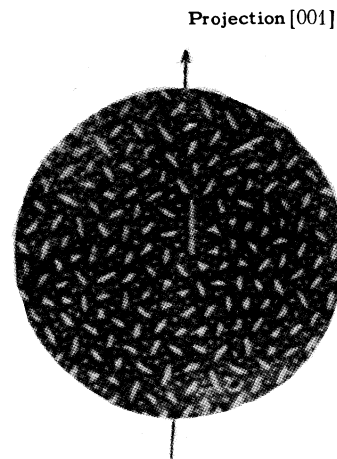


FIG. 5

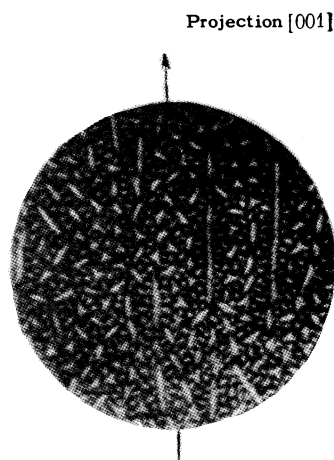


FIG. 6

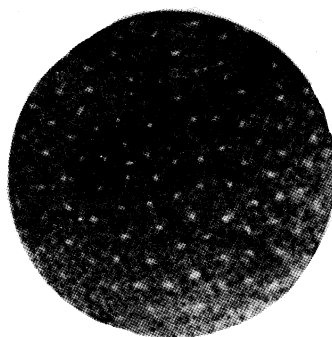


FIG. 7

FIGS. 3–7. Photographs of structures of the intermediate state. White regions are superconducting. Field of view 1.4 cm in diameter. The arrows denote the projections of the crystallographic axes onto the plane of the specimen.

FIG. 3. Specimen 1. $T = 3.04^\circ$, $C_s = 0.08$.

FIG. 4. Specimen 2. $T = 3.24^\circ$, $C_s = 0.17$.

FIG. 5. Specimen 9. $T = 3.00^\circ$, $C_s = 0.17$.

FIG. 6. Specimen 9. $T = 3.00^\circ$, $C_s = 0.17$.

The transition to the intermediate state produced by cooling.

FIG. 7. Filament-like s domains. $T = 3.00^\circ$, $C_s = 0.06$.

on the surface of the specimen as elongated spots, having one or several directions of preferred orientation (Figs. 3–5).

From the condition that the free energy of the system should be a minimum, it follows that in the body of the specimen the s domains must have a cross section approaching circular (with minimum surface area), flattening only at the surface of the specimen (like the end of a screw-driver). This is due to the reduced magnetic field energy, compared with the case of cylindrical regions with the same cross section. For $C_s \rightarrow 0$ the observed dimensions of the s domains decrease and no flattening takes place near the surface (see Fig. 7).

When C_s increases, small specks of s phase appear in the structures (the white dots in Figs. 4–6), which are, apparently, a peculiar form of branched structure, also leading to a reduction of magnetic energy.⁴

For $C_s > 0.2$ the structures take on a more involved character, going over for $C_s \rightarrow 1$ to a system of wrinkled n domains.¹

To explain the results obtained we must first discuss the factors that can affect the orientation of the s domains, apart from the anisotropy of Δ which interests us.

1. The movement of the ns boundaries leads to the production of local eddy currents flowing near the boundaries and hindering the movement. In pure metals, as Faber has shown,⁵ the electron mean free path exceeds the thickness of the layer in which the eddy currents flow, i.e., the conditions are analogous to the conditions for the anomalous skin effect. The anisotropy in the rate of growth of the s domains will therefore be related to the anisotropy of the anomalous skin effect in a given metal.

We can judge the influence of this factor by comparing Figs. 5 and 6. In one case (Fig. 6) the

specimen was brought into the intermediate state from the normal state. The supercooling produced a rapid growth of long s filaments parallel to the $[001]$ axis. In the second case (Fig. 5) the specimen was originally in the intermediate state, with larger C_s and with a finely dispersed structure. On heating to the required temperature the s domains gradually "crystallized out" in the presence of sufficient nuclei. In this case layers parallel to the $[001]$ axis were encountered very rarely. We made analogous observations on other specimens. We then have grounds for saying that for such a transition the influence of eddy currents on the anisotropy of the structure is small.

We therefore used the second method of transition in all the remaining cases, sometimes also applying a slow temperature oscillation with amplitude $\sim 0.01^\circ$, which improved the regularity of the structures.

2. One can also assume an ordering of the structure to result from a correlation in the orientation of the s domains relative to one another, i.e., some "packing" of the domains due to their magnetic interaction. The following facts, however, contradict this suggestion: a) the structures in specimens with different crystal orientations differ from one another, b) in structures of the type shown in Fig. 3, one finds neighboring regions oriented perpendicular to one another as often as parallel, c) the orientation of the s domains is related to the direction of the crystal axes in the specimen.

From the above we deduce that the observed preferred orientation of the s domains is determined primarily by the anisotropy of Δ .

Results obtained with the "frozen-in flux" method. We counted on the photographs the number of regions whose directions lay in consecutive equal intervals of angle, and plotted polar diagrams (Figs. 8–10 and 13–15) showing the corresponding number in the direction of the normal

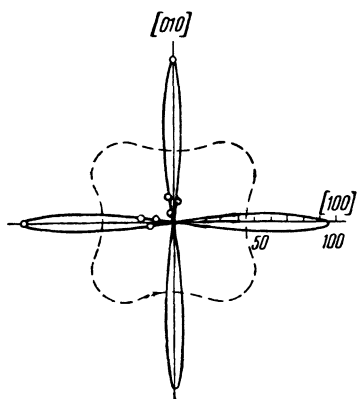
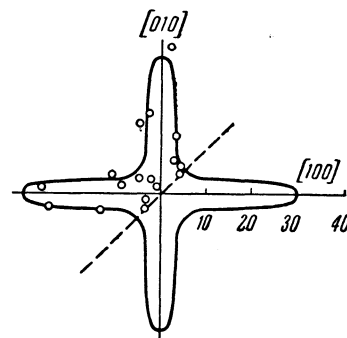


FIG. 8. Specimen 1.
 $T = 3.04^\circ$, $C_s = 0.08$.
Angular interval 10° .

FIG. 9. Specimen 1.
 $T = 3.52^\circ$, $C_s = 0.12$.
Angular interval 10° .



to the elongated side of the s domain (this direction will be referred to as n in what follows). The part of the diagram between 180 and 360° is just a duplicate of the $0 - 180^\circ$ part. The scale for the number of regions is shown along one of the radii. The appearance of the diagram is independent of C_s for a given specimen.

We shall consider first the results of experiments for the simplest orientations of the crystallographic axes relative to the specimen surface, and at a temperature relatively far from the critical temperature ($T \sim 3^\circ\text{K}$).

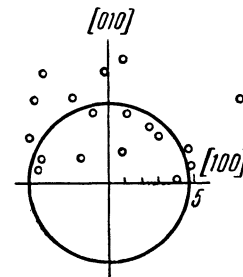
1. Specimen 1. The normal to the surface of the specimen N directed along the 4-fold crystal axis $[001]$. The s domains are equally divided between the equivalent directions $[100]$ and $[010]$ (Figs. 3 and 8). The corresponding polar diagram for $\Delta(n)$ must have two identical minima in these directions, i.e., it must have the form of the dashed curve shown in Fig. 8.

2. Specimen 2 (Fig. 4). The normal N close to the $[100]$ axis in direction. The greater part of the s domains is elongated along the $[001]$ axis, but about 15% have a perpendicular direction. It is natural to assume that the polar diagram for Δ would have, in this case, two minima, one of which is wider and deeper than the other.

3. Specimen 6. The normal N parallel to the $[110]$ axis. There are again two preferred orientations along the $[001]$ and $[110]$ directions with roughly the same number of domains.

Figure 11 shows how the structure changes as N varies from the $[100]$ to the $[110]$ direction.

FIG. 10. Specimen 1. $T = 3.60^\circ$,
 $C_s = 0.16$. Angular interval 10° .



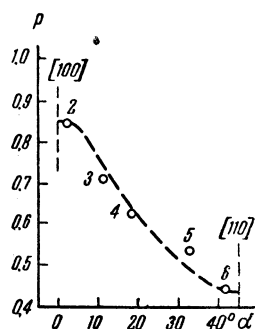


FIG. 11. p — the ratio of the number of domains elongated along the $[001]$ axis, to the total number. The domains are oriented either along the $[001]$ axis or perpendicular to it. The numbers at the points denote the specimen number. $T = 3^\circ$ K, $C_s = 0.1-0.2$, α is the angle between the $[100]$ axis and the surface of the specimen.

The magnitude of Δ must in general depend on the direction of the normal \mathbf{n} to the ns boundary and the direction \mathbf{l} of the superconductivity current in the boundary layer, i.e., on three angular parameters, in so far as $\mathbf{l} \perp \mathbf{n}$.

Each of the experiments described makes possible a comparison of the values of Δ , for a given direction of \mathbf{N} , associated with ns boundaries when $\mathbf{n} \perp \mathbf{N}$ and $\mathbf{l} \perp \mathbf{N}$.

We must have additional data, obtained by other methods, in order to connect together the data for specimens with different \mathbf{N} . In the second part of this work we shall return to this question, but for now, to systematize our qualitative data, we shall make the simplifying assumption that the dependence $\Delta(\mathbf{i})$ for a given \mathbf{n} is small and can be neglected compared with the variation of $\Delta(\mathbf{n})$.

With this assumption we can describe the $\Delta(\mathbf{n})$ surface qualitatively from our data. Its central sections by planes parallel to the surfaces of the specimen must look like the polar diagrams of Δ for the corresponding experiments.

There is apparently a minimum on the $\Delta|\mathbf{n}|$ surface for $\mathbf{n} \parallel [100]$, since there are minima at this point for two mutually perpendicular sections of the surface by its plane of symmetry (see above, items 1 and 2).

It follows in an analogous way from item 2 (or 3) that for $\mathbf{n} \parallel [001]$ there is a shallower minimum on the surface i.e. $\Delta_{[001]} > \Delta_{[100]}$. These

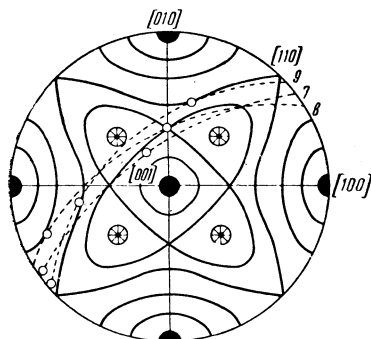
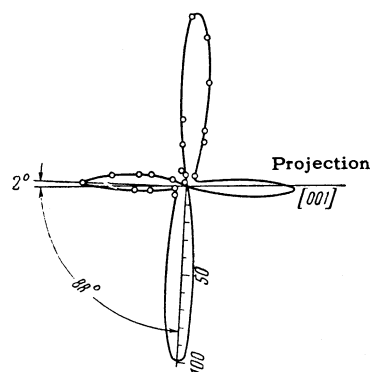


FIG. 12

FIG. 13. Specimen 7. $T = 3^\circ$. Data from four photographs: $C_s = 0.16$; 0.14 ; 0.14 ; 0.13 . Angular interval 5° .



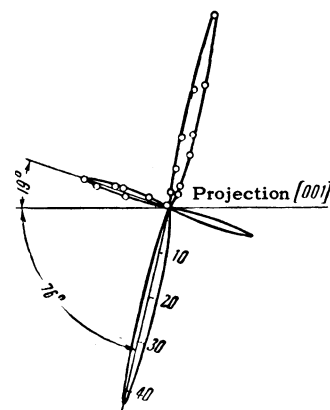
minima are indicated by full circles in the stereographic projection of Fig. 12. The point $[110]$ on the $\Delta(\mathbf{n})$ surface must be the saddle point, according to items 1 and 3.

We should point out that an attempt to represent the results by using the $\Delta(\mathbf{i})$ surface, neglecting the dependence of $\Delta(\mathbf{n})$, would immediately lead to an inconsistency, since then

$$\begin{array}{llll} \text{from item 1 it follows that} & \Delta^{[110]} > \Delta^{[100]} \\ \text{" " 3 " " " " } & \Delta^{[110]} \approx \Delta^{[001]} \\ \text{" " 2 " " " " } & \Delta^{[001]} < \Delta^{[100]} \end{array}$$

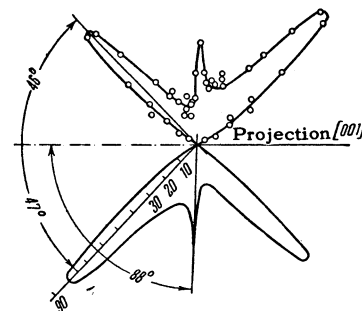
where the superscript to Δ denotes the direction of the superconductivity current.

FIG. 14. Specimen 8. $T = 2.95^\circ$. $C_s = 0.14$. Angular interval 2° .



The form of the $\Delta(\mathbf{n})$ surface can be determined on the basis of experiments with specimens 7, 8, and 9 (Figs. 13–15). The circuits corresponding to the surfaces of these specimens are

FIG. 15. Specimen 9. $T = 3^\circ$. Data from four photographs: $C_s = 0.17$; 0.15 ; 0.09 ; 0.08 . Angular interval 3° .



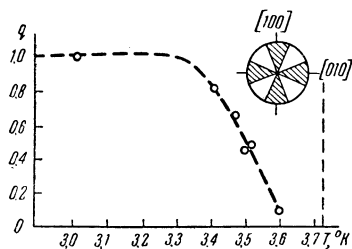


FIG. 16. Specimen 1. $q = (a - b)/(a + b)$, where a is the number of s domains with normals making angles of less than 22.5° with the $[100]$ or $[010]$ axis, i.e., falling within the shaded sectors of the diagram; b is the number of remaining s domains. $C_s = 0.1 - 0.2$.

shown by dashes in Fig. 12, and the points for the relative minima of Δ in these sections (corresponding to the peaks of Figs. 13 – 15) are shown by the small circles. If we represent the dependence $\Delta(\mathbf{n})$ by using lines of constant Δ , then these lines must touch the dashed curves at the points of relative minimum.

The arbitrariness in drawing the lines of constant Δ turns out to be insignificant in practice.

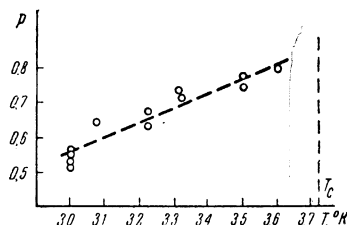
The lines of equal Δ , shown in Fig. 12 and obtained from the data on the positions of the peaks in Figs. 13 – 15, also explain a number of other features of these diagrams. For example, the large difference in height between the peaks in Fig. 14 is related to the fact that one of the minima for specimen 8 in Fig. 12 (near the saddle point) lies between two close maxima, and the probability of the s domain falling in this narrow angular interval is small.

The diffuseness and the sharp asymmetry in the form of the peaks in Fig. 15 are related to the fact that the circuit for specimen 9 in Fig. 12 runs almost exactly along a line of constant Δ far from the $[001]$ axis, and spreads through the maximum in the region between the peaks near the $[001]$ axis.

Let us examine the temperature dependence of the anisotropy of Δ . The data obtained with specimen 1 ($\mathbf{N} \parallel [001]$) show that the anisotropy in this section gradually decreases as $T \rightarrow T_C$. With increasing temperature, the polar diagrams of the distribution of s domains become ever more diffuse (see Figs. 8 – 10 and 16). At $T = 3.6^\circ\text{K}$ the distribution is practically isotropic, since the disordering action of other factors predominates over the anisotropy of Δ at this temperature.

On the other hand, we found no noticeable temperature dependence for the structures obtained for $\mathbf{N} \parallel [100]$ up to 3.6°K . The structures obtained with $\mathbf{N} \parallel [110]$ approach the structures for

FIG. 17. Specimen 5. p is the ratio of the number of domains elongated along the $[001]$ axis to the total number; $p = 0.5$ corresponds to equal probability of the two different directions. $C_s = 0.1 - 0.2$.



$\mathbf{N} \parallel [100]$ for $T \rightarrow T_C$ (see Fig. 17) and become practically identical at $T = 3.6^\circ$. It became difficult to observe the structures at $T = 3.6^\circ$ because of the small contrast in the pictures (due to the small field H_C), and it was not possible to raise the temperature further.

From our observations we can deduce that for $T \rightarrow T_C$ the $\Delta(\mathbf{n})$ surface takes on the symmetry of a body of rotation and has a line of minima on the equator. The question of whether the small minimum at the pole is preserved or merges into the maximum is still open.

We will return to a discussion of these results after presenting the second part of the work.

2. TORSION BALANCE METHOD

An anisotropy in Δ must lead to a dependence of the free energy, F , of the specimen in the intermediate state on the direction of the magnetic field relative to the crystallographic axes of the specimen.

If the specimen is hung on a taut thread in a horizontal magnetic field, then by measuring the angle turned through by the thread at equilibrium the mechanical moment $M = -\partial F/\partial \alpha$ can be determined, where α is the angle turned through by the specimen around a vertical axis. The magnitude of M must be related to the anisotropy of Δ if, of course, the specimen is sufficiently uniform and the "dry friction" forces and irregularities in the external shape of the specimen have no effect.

In our experiments we studied single crystal specimens of tin which were close to spherical in shape. The specimens were cast in a glass former and the deviations from spherical were $2 - 3 \mu$ in diameter for a mean diameter of about 12.6 mm . After cooling to helium temperatures the specimens approximated to an oblate ellipsoid of revolution with axes differing by 0.1 mm .

The torsion balance, used for measuring the mechanical moment in the intermediate state, was also used to measure the conductivity of metal specimens at helium temperatures (including all the specimens mentioned below) and has been described elsewhere.⁶

TABLE I.

Specimen No.	$10^{10}\rho_0$, $\Omega \cdot \text{cm}$	Impurity Content, %	$10^4 m _{\max}$ (at $T = 3.69^\circ$)
I	1c	$< 6 \cdot 10^{-5}$	4
	2c	$8 \cdot 10^{-5}$	3
	3c	$3 \cdot 10^{-4}$	5
	4c	$3 \cdot 10^{-4}$	3
II	5c	$< 6 \cdot 10^{-5}$	11, 14*
	6c	$8 \cdot 10^{-5}$	8
	7c	$1 \cdot 10^{-4}$	10
	8c	$2 \cdot 10^{-3}$	12
	9c	$3 \cdot 10^{-3}$	8

*Two measurements on different days.

The measurements were carried out in the following way. After the required temperature had been established, a small field H_S was switched on and the mechanical moment in the superconducting state, M_S , was determined. This moment is related to the deviation of the specimen from a spherical shape, already mentioned. We then determined the critical field H_C by reducing the field gradually to a value $(2/3)H_C$, at which the specimen went over from the intermediate into the superconducting state. This transition was determined by finding when the specimen ceased being carried by the slowly rotating field which induces eddy currents in the normal phase. The specimen was then put into the intermediate state and the moment of the forces acting on it was measured for different directions of the magnetic field in the horizontal plane. All but some preliminary measurements were made at the concentration $C_S = 0.5$, i.e. for $H = (5/6)H_C$.

We took each point twice in order to annul the influence of "dry friction." In one case the specimen, previously inclined to the position of equilibrium, approached it by turning in a clockwise direction, and in the other case by turning in the opposite direction. As far as possible, all conditions were symmetrical in both cases. The approach to the equilibrium position was made very slowly (to prevent eddy currents) and usually took 5–6 min. The position reached by the specimen when approaching from different directions did not coincide, and this served as a measure of the magnitude of the "dry friction." We took the mean of the results of the two measurements as the position for true thermodynamic equilibrium. From the value of the moment M obtained, we subtracted the part M_e which was caused by the specimen not being spherical. M_e was determined from the moment M_S in the superconducting state for the same magnetic field direction, using

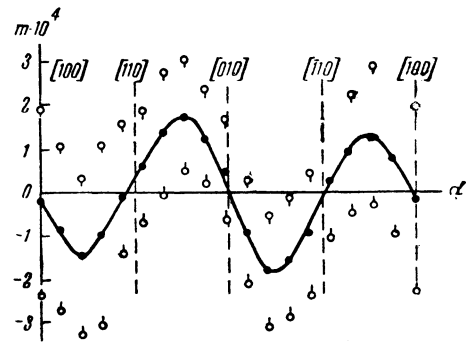


FIG. 18. Spherical specimen 1c. Axis of rotation along [001], $T = 3.11^\circ$.

the formula $M_e = 4M_S (H_C - H)^2/H_S^2$, which can easily be derived by assuming the specimen to be an ellipsoid that differs little from a sphere. The difference obtained $M - M_e = M_i$ is the quantity required, related to the anisotropy of the structure in the intermediate state. The effect observed was small, so that M_e and M_i were of the same order of magnitude. The deflection of the light spot of the torsion balance was usually not more than 5–10 mm and its position was determined with an accuracy of 0.1 to 0.2 mm.

Results obtained with the torsion-balance method. We studied nine specimens, the residual resistance ρ_0 and the presumed purity of which are shown in the first and second columns of Table I. It appeared that the specimens could be divided into two qualitatively different groups according to the type of curves obtained (group I comprising specimens 1c–3c and group II specimens 5c–9c). Within the groups, the differences were more of a quantitative nature.

Specimen 4c was intermediate in its properties.

We shall discuss the properties of specimens of the first group, which appear to approximate more closely to the properties of an ideal uniform single crystal. Specimens 1c and 2c were comparatively similar and gave results in close agreement.

One of the curves obtained with specimen 1c is shown in Fig. 18. The specimen was hung so that the [001] axis was vertical. The abscissa represents the angle, α , between the [100] axis and the magnetic field. The orientation of the specimen relative to the balance was determined by x-ray diffraction. The ordinate gives the mechanical moment $m = 8\pi M_i/H_C^2 V$, where V is the volume of the specimen. The circles show the results of measurement when the equilibrium position is approached from two directions (with a correction for departures from sphericity) and

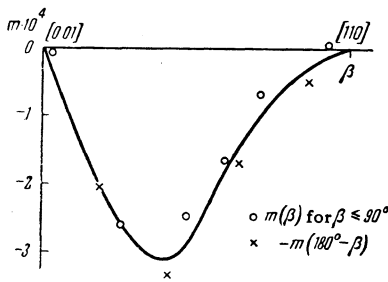


FIG. 19. Spherical specimen 1c. Axis of rotation along $[1\bar{1}0]$, $T = 3.13^\circ$. Points obtained by averaging over the approach from the left and from the right.

the solid dots and the curve represent the mean. It can be seen from the figure that the moment of the "dry friction" forces Δm (i.e., the distance between the upper and lower points) does not depend on direction in a regular way, while the mean moment changes with angle smoothly and is symmetrical with respect to the crystallographic directions.

Assuming that the mean value of m is the equilibrium value, we obtain, apart from an arbitrary constant, $f(\alpha) = -\int m d\alpha$, where f is the free energy of the specimen divided by $VH_C^2/8\pi$. For $H \parallel [110]$ f is a maximum; it is a minimum for $H \parallel [100]$. For specimen 1c at $T = 3.11^\circ$ $f_{[110]} - f_{[100]} = 7.4 \times 10^{-5}$, where the subscript denotes the direction of the magnetic field.

Figures 19 and 20 show the curves obtained on the same specimen at 3.13° for the cases where the $[110]$ and $[100]$ axes were vertical. Integrating these curves gives $f_{[110]} - f_{[001]} = 25 \times 10^{-5}$ and $f_{[010]} - f_{[001]} = 21 \times 10^{-5}$. The difference between these two values is 4×10^{-5} , which agrees in sign and order of magnitude with the value 7.4×10^{-5} , derived from Fig. 18. For specimen 2c at $T = 3.13^\circ$ the difference $f_{[010]} - f_{[001]} = 23.6 \times 10^{-5}$.

In order to connect these results with the anisotropy of Δ , we have to make some assumptions about the structure of the intermediate state of spherical specimens.

Experiments made by the powder method¹ have shown that a sphere in the intermediate state with $C_S = 0.5$ has a radial layer structure in the region of the magnetic equator and a complicated wrinkled structure elsewhere.

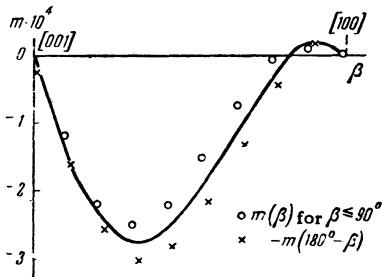


FIG. 20. Spherical specimen 1c. Axis of rotation along $[010]$, $T = 3.13^\circ$. Points obtained by averaging over the approach from the left and from the right.

If we construct the normals to all the surfaces of separation of the phases within the sphere, their traces on a stereographic projection will appear in a narrow band running along the magnetic equator, since it is known that inside a sphere the field has a constant direction at all points. In what follows we shall assume that the normals lie exactly in the plane of the magnetic equator, that all directions in this plane are equally represented, and that the free energy in the intermediate state is determined by the value of $\overline{\Delta(n)}$, averaged over these directions. It is not difficult to see that with these assumptions the data for f are in qualitative agreement with the form of the $\Delta(n)$ surface, shown in Fig. 12, since averaging Δ over the great circle (110) must lead to a larger value of Δ than the circle (100) , and the average over (001) to a smaller value of Δ .

For a quantitative measure of the anisotropy of Δ we need the absolute value of the free energy in the intermediate state. Using Landau's model for the structure of the intermediate state,⁷ an expression can be derived for the free energy of a sphere: $f = 2\sqrt{2}\varphi\Delta/R$, where R is the radius of the sphere and $\varphi = 0.0221$ for $C_S = 0.5$ *. Substituting Δ for tin here, equal to $2.3 \times 10^{-5} (1 - T/T_C)^{-1/2}$ cm (see references 2 and 8), we obtain $f = 2.6 \times 10^{-3} (1 - T/T_C)^{-1/4}$. For specimen 1c at 3.13° , for example, we then derive $(f_{[100]} - f_{[001]})/f \approx 6\%$.

Since $f \sim \sqrt{\Delta}$, the corresponding relative change in Δ must be twice as great i.e. 12%. The change in the unaveraged value of Δ must be even greater. A rough calculation based on the assumptions about the way of averaging Δ shows that the relative difference between the maximum value, at the points shown in Fig. 12 by stars, and the minimum at the points $[100]$ is 20–25% at $3.1^\circ K$.

*For the calculation it was assumed that the n domains in a sphere are not branched and are distributed in a radial direction. It was also taken into account that the lines of force make an angle with the surface of the sphere which depends on the magnetic latitude. If the sphere is divided into strips by coaxial cylinders, then the energy enclosed in such a strip per unit surface of the sphere is $F = (H_C^2/2\sqrt{2}\pi) \times \sqrt{\varphi(C_S)\Delta R} \sin^2 \vartheta$, where ϑ is the latitude (see reference 2). Integration of this expression gives the formula above. Calculation according to reference 4 shows that neglecting the branching of the layers does not lead to any appreciable error in our case in calculating the free energy (an error of ~10% in the worst conditions, far from T_C). We obtain for the period of the structure the expression $a = \sqrt{2R\Delta\varphi}$, independent of latitude. This expression also holds for a cylinder in a transverse field.

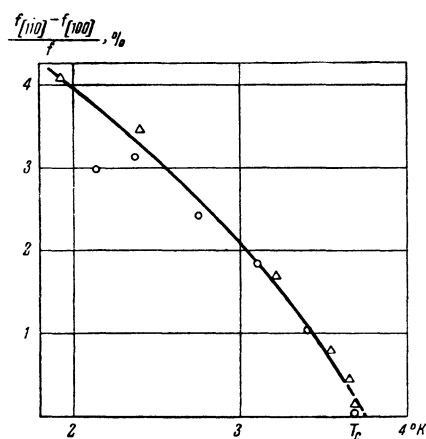


FIG. 21. Rotation about the [001] axis. O — specimen 1c, Δ — specimen 2c.

The temperature dependence of the effect was different for the various orientations of the specimen in the balance. For rotation around the [001] axis the shape of the curves did not change appreciably with temperature, while the amplitude of the curves and the ratio $(f_{[110]} - f_{[100]})/f$ tended to zero for $T \rightarrow T_c$ (see Fig. 21). The curve of Fig. 21 represents, in more accurate form, the behavior also derived by the "frozen-in flux" method (see Fig. 16).

For rotation about the [100] and [110] axes the shape of the curves was slightly different at temperatures far from and close to T_c . The ratios $(f_{[010]} - f_{[001]})/f$ and $(f_{[110]} - f_{[001]})/f$ were little dependent on temperature and apparently tended to a limiting value for $T \rightarrow T_c$ (see Table II). We should note that the experimental conditions for a temperature near T_c were worse than for a temperature far from it, and the reproducibility and accuracy of the curves deteriorated. The difference of 2×10^{-2} between $(f_{[110]} - f_{[001]})/f$ and $(f_{[010]} - f_{[001]})/f$ at $T = 3.69^\circ$ comes from the poor reproducibility of the data, in so far as careful direct measurements give $(f_{[110]} - f_{[100]})/f < 0.3\%$. The reason for these disagreements is apparently related to the presence of some sort of lattice defects, the influence of which is more apparent near T_c . An analogous phenomenon was

found in the same form with the specimens of group II (5c — 9c).

The rather complicated behavior of the specimens of group II is apparently connected with their imperfection, and we will only discuss them briefly to help in substantiating the results obtained with specimens of group I.

The curves obtained for specimens 5c — 9c at $T = 3.69^\circ$ with rotation about the [100] axis were very different from the corresponding curves for the specimens of group I. The value of m became zero in the [001] and [010] directions and at an intermediate point, $\beta = 30 - 40^\circ$ (β is the angle with the [001] axis), which was a point of stable equilibrium. The maximum value of $|m|$ was 2 — 4 times greater than $|m|_{\max}$ for the specimens of group I (see Table I).

The resemblance between the curves obtained with some of the group II specimens led us at first to the incorrect conclusion⁹ that the effect is related to the anisotropy of Δ . It was only after we had managed to obtain the group I specimens that we finally established that the real reason for these curves is apparently the chance plastic deformation of the specimens and the formation of regions with somewhat different values of H_c .

This conclusion is borne out by the following facts:

a) For $T \sim 3^\circ$, far from T_c , this effect disappears and the curves for rotation about the [100] and [001] axes agree well with the corresponding curves for group I specimens. The relative indeterminacy in the value of H_c must, in fact, decrease with decreasing temperature, since its absolute value is little dependent on T (cf. the data of reference 10).

b) The effect stays at an appreciable magnitude for $C_s \ll 0.5$ (being halved only at $C_s = 0.04$) and is thus connected with a small fraction of the volume of the specimen.

c) A small plastic deformation (rolling it

TABLE II.

T°, K	Specimen No.	Rotation about the [001] axis			Rotation about the [110] axis		
		$10^4 m _{\max}$	$10^4 \overline{\Delta m}^*$	$(f_{[010]} - f_{[001]})/f, \%$	$10^4 m _{\max}$	$10^4 \overline{\Delta m}^*$	$(f_{[110]} - f_{[001]})/f, \%$
3.69	1c	4	1	4.1	4.5	3.4	6.2
3.69	2c	3	1.1	3.7	—	—	—
3.69	3c	5	6	5.4	—	—	—
3.13	1c	2,7	1.5	5.1	3.1	1.6	6.1
3.13	2c	3	0.9	5.7	—	—	—
2.08	1c	—	—	—	3	3.8	4.7

* $\overline{\Delta m}$ is the average value of the "dry friction" forces, i.e., the mean of the difference in the values of m when the equilibrium position is approached from different directions.

lightly on the top of a table) of specimen 4c led to an increase of $|m|_{\max}$ at $T = 3.69^\circ$ to 50×10^{-4} , i.e. a 16-fold increase.

The observations described lead us to suppose that the anomalous behavior of the group II specimens is to be explained by the existence of some regions of twinning in them. The mechanical twinning plane in tin (301) lies at an angle of $\sim 30^\circ$ to the [001] axis, which is close to the equilibrium direction of the domains in the specimens of group II.

It seems that measurement of the forces acting on a specimen in the intermediate state might be applicable for showing up small lattice defects, which can not be found by other methods.

The difference between the properties of specimens of groups I and II for T close to T_C serves as some confirmation that the anisotropy of the group I specimens in the intermediate state is not related to lattice imperfections, and is due to the anisotropy of surface tension.

3. DISCUSSION OF RESULTS

A. Comparison of the different methods of studying the anisotropy of Δ . A comparison of the results obtained by the two methods described above shows that they are in satisfactory agreement and partly complement each other. The "frozen-in flux" method enables one to build up a qualitative picture of the anisotropy of Δ at temperatures far from T_C , which is confirmed by the data obtained with the torsion balance. We should point out that these two methods are independent, since in the first the energies of separate domains within one structure are compared for a given magnetic field direction, while in the second the energies of a structure as a whole are compared for different field directions.

A consideration of the results obtained by both methods leads to the conclusion that, in the temperature range studied, the dependence of Δ on the direction of the normal to the surface of separation is greater than the dependence on the current direction. In any case, the dependence $\Delta(\mathbf{n})$ derived is quite enough to explain all the observations, while consideration of the dependence $\Delta(\mathbf{i})$ alone, neglecting the dependence on \mathbf{n} , leads to inconsistencies. This deduction, for a temperature of 3°K , was made in the first part of this work. Near T_C the "frozen-in flux" method shows only that the orientation of layers with $\mathbf{n} \perp [001]$ and $\mathbf{i} \parallel [001]$ are more favorable, i.e., that the surface of $\Delta(\mathbf{n})$ is prolate, or that of $\Delta(\mathbf{i})$ is oblate, in the [001] direction. The

torsion balance method yields $f_{[100]} - f_{[001]} > 0$, from which it follows that the surface of $\Delta(\mathbf{n})$ or $\Delta(\mathbf{i})$ is drawn out. For agreement between the results we must therefore introduce a dependence $\Delta(\mathbf{n})$.

The nature and magnitude of the dependence of Δ on the current direction can only be decided experimentally from a more detailed and exact quantitative investigation of the anisotropy of Δ . In principle this could be achieved by measuring the period of the structures in a flat specimen located in an inclined magnetic field. It would be a fairly difficult task to carry out these measurements with sufficient accuracy and completeness, and might only be undertaken after a preliminary qualitative study.³

B. Comparison of the results with theory. It seems to us that the most important result from the theoretical point of view is the anisotropy of Δ found in the (001) plane, perpendicular to the four-fold symmetry axis of the crystal. A theory based on the existence of a local tensor relation between current and field, should for such a high degree of symmetry lead to the absence of anisotropy in this plane (see Ginzburg and Landau^{11,12}). The existence of anisotropy is evidence of the existence of a non-local correlation between current and field in a superconductor.

The existence of such a correlation, predicted by Pippard,¹³ is one of the main points of the microscopic theory of superconductivity due to Bardeen, Cooper, and Shrieffer¹⁴ and to Bogolyubov.¹⁵ The electrodynamics of anisotropic superconductors, taking into account such a correlation, has not yet been worked out. We cannot, therefore, compare our results with data on the anisotropy of other properties of superconductors, especially since such information is very scanty. Bezuglyi et al.¹⁶ and Morse et al.¹⁷ have investigated the anisotropy in the absorption of sound in tin, and Pippard¹⁸ and Schawlow and Devlin¹⁹ have studied the anisotropy of penetration depth δ .

It appears that the gradual disappearance of the anisotropy of Δ in the (001) plane, as the temperature approaches T_C , is related to the increase in thickness of the transition layer between the phases, equal to Δ in order of magnitude, as compared with the parameter ξ that characterizes the distance over which a non-local correlation exists. In so far as ξ is independent of temperature, $\xi/\Delta \sim \sqrt{T_C - T}$ for $T \rightarrow T_C$. As can be seen from Fig. 21, $(f_{[110]} - f_{[100]})/f$ tends to zero apparently linearly with $T_C - T$. Thus

$$(\Delta_{[110]} - \Delta_{[100]})/\Delta \sim (\xi/\Delta)^2 \text{ for } T \rightarrow T_C.$$

For small ξ/Δ the connection between current and field can be considered local and the relation between the anisotropy of Δ and δ can be found from the phenomenological theory of Ginzburg and Landau. The anisotropy of superconductivity can then be described by introducing the effective mass tensor for the superconducting electrons.¹² We confine ourselves to the simplest case, when the normal to the phase boundary is directed along one of the principal axes of the mass tensor, z , and the current flows along another principal axis x .

In the isotropic case $\Delta = \delta_0 \alpha(\kappa)/\kappa$ where δ_0 is the penetration depth for $H \rightarrow 0$, and²⁰ $\kappa = 4.32 \times 10^7 H_C \delta_0^2$. Values of $\alpha(\kappa)/\kappa$ were tabulated by Ginzburg,²¹ and $\alpha(\kappa) \rightarrow 1.89$ for $\kappa \rightarrow 0$.

It can be shown easily that in the anisotropic case

$$\Delta_z^x = \delta_{0x} \alpha(\kappa_z)/\kappa_{xz},$$

where $\kappa_{xz} = 4.32 \times 10^7 H_C \delta_{0x} \delta_{0z}$, $\delta_{0k} = (m_k c^2 / 4\pi e^2 n_s)^{1/2}$, m_k is the effective mass along the principal axis k , and n_s is the concentration of superconducting electrons. Thus $\Delta_z^x \sim \alpha(\kappa_{xz}) \delta_{0z}$ and since α is relatively weakly dependent on κ , Δ_z^x is mainly determined by the effective mass and by the direction of the normal to the phase interface.

For tin

$$\frac{\partial \Delta_z^x}{\partial \delta_{0z}} \delta_{0z} \bigg/ \frac{\partial \Delta_z^x}{\partial \delta_{0x}} \delta_{0x} \approx 3.5,$$

i.e. the dependence of Δ_z^x on δ_{0x} is 3–4 times less than the dependence on δ_{0z} . Our data confirm this result qualitatively.

It will be possible to compare our results quantitatively with these relations when we have data on the temperature dependence of the anisotropy of Δ for $T_C - T \sim 0.1 - 0.01^\circ$, where the tensor representation of the anisotropy is applicable.

We are very grateful to Academician P. L. Kapitza for his interest in the work and to A. I. Shal'nikov for a detailed discussion of the results.

¹ B. M. Balashova and Yu. V. Sharvin, JETP **31**, 40 (1956), Soviet Phys. JETP **4**, 54 (1957).

² Yu. V. Sharvin, JETP **33**, 1341 (1957), Soviet Phys. JETP **6**, 1031 (1958).

³ A. G. Meshkovskii, JETP **19**, 54 (1949).

⁴ E. M. Lifshitz and Yu. V. Sharvin, Dokl. Akad. Nauk. SSSR **79**, 783 (1951).

⁵ T. E. Faber, Proc. Roy. Soc. **A223**, 174 (1954).

⁶ V. B. Zernov and Yu. V. Sharvin, JETP **36**, 1038 (1959), Soviet Phys. JETP **9**, 737 (1959).

⁷ L. D. Landau, JETP **7**, 371 (1937).

⁸ Yu. V. Sharvin, JETP **38**, 1 (1960).

⁹ Yu. V. Sharvin and V. L. Sedov, JETP **29**, 897 (1955), Soviet Phys. JETP **2**, 771 (1956).

¹⁰ Kan, Lazarev, and Sudovtsov, JETP **18**, 825 (1948).

¹¹ V. L. Ginzburg and L. D. Landau, JETP **20**, 1064 (1950).

¹² V. L. Ginzburg, JETP **23**, 236 (1952).

¹³ A. B. Pippard, Proc. Roy. Soc. **A216**, 547 (1953).

¹⁴ Bardeen, Cooper, and Schrieffer, Phys. Rev. **108**, 1175 (1957).

¹⁵ N. N. Bogolyubov, JETP **34**, 58 (1958), Soviet Phys. JETP **7**, 41 (1958).

¹⁶ Bezuglyi, Galkin, and Korolyuk, JETP **36**, 1951 (1959), Soviet Phys. JETP **9**, 1388 (1959).

¹⁷ Morse, Olsen, and Gavenda, Phys. Rev. Letters **3**, 15 (1959).

¹⁸ A. B. Pippard, Proc. Roy. Soc. **A203**, 98 (1950).

¹⁹ A. L. Schawlow and G. E. Devlin, Bull. Am. Phys. Soc. **4**, 224 (1959).

²⁰ L. P. Gor'kov, JETP **36**, 1918 (1959), Soviet Phys. JETP **9**, 1364 (1959).

²¹ V. L. Ginzburg, JETP **30**, 593 (1956), Soviet Phys. JETP **3**, 621 (1956).